Egyptian Journal of Aquatic Biology and Fisheries
Zoology Department, Faculty of Science,
Ain Shams University, Cairo, Egypt.
ISSN 1110 – 6131
Vol. 26(1): 505 – 531 (2022)
www.ejabf.journals.ekb.eg

Hard engineering coastal structures; detrimental or beneficial: A case study of Agami−Sidi Kerair coast, Mediterranean Sea, Egypt

Esraa A. El-Masry
Department of Oceanography, Faculty of Science, Alexandria University, Alexandria, Egypt
E-mail: esrasero@yahoo.com
ORCID No.: 0000-0003-3555-986X

ARTICLE INFO
Article History:
Received: July 30, 2021
Accepted: Dec. 19, 2021
Online: Feb. 23, 2022

Keywords:
Shoreline change rate,
DSAS,
GIS,
Landsat,
Protection structures,
Beach nourishment

ABSTRACT
This study was conducted to conjugate geospatial technology with Digital Shoreline Analysis System (DSAS) to monitor, analyze, and quantify the impacts of hard structures on the spatiotemporal shoreline dynamics along Agami−Sidi Kerair coastal" Pilot" area over the last 25 years (1995–2020). The results revealed that the study area lost about 63.78 % (erosion) of the beach area while gaining about 36.22 % of the beach area (accretion). During 1995–2020, Agami–Sidi Kerair shoreline experienced an accretion with an average rate of 0.56 m/year (End Point Rate, EPR) and 1.00 (Linear Regression Rate, LRR), reaching a maximum rate of 3.19 m/year (EPR) and 4.30 m/year (LRR). The shoreline analysis showed that applying hard defenses for the study area is detrimental since they convey the shoreline retreat and the beach erosion problem to the adjacent areas. In addition, they disturb sediments supply and accelerate the bottom erosion in front of them, causing downdrift scouring as a barrier to the longshore sediments transport. Furthermore, the grown level of negative consequences would cause hazardous rip current increasing the potential for drownings. Moreover, they are expensive and require costly ongoing maintenance.

1. INTRODUCTION

Erosion along the Mediterranean coast of Egypt (approximately 1066 km) has become a serious problem, rising in magnitude and dominance; this has been recognized and documented. Egypt has an earlier experience using the traditional hard engineering coastal protection, particularly along the Mediterranean coast of Egypt. One of the oldest and documented hard structures is the Muhammed Ali Seawall established in 1830, to the east of Alexandria city (west of Abu Qir Bay) to protect the coast in this area against flooding and overtopping.

Later, the application of hard structures continued with the undergoing serious erosion problems, mainly along the Nile delta coast and its headlands. These conditions have prompted the authorities and developers to establish protection means to mitigate the effect of erosion and sometimes create sheltered beaches for holidaymakers and water

activities. Subsequently and during the early 20th century, hard engineering structures were the only management strategy to encounter the erosion problems on the northern Nile delta and the Northwestern newly developed urban and tourism structures along the Mediterranean coast. The main type of these structures includes groins; breakwaters whether detached or connected to the shore, emerged, or submerged; seawalls parallel to the coastline and revetments. Nevertheless, these hard structures may cause erosion and accretion in the down and up drifts, respectively **(El Sayed, 2017)**. These were observed and documented in the coastal protection works at the Mediterranean Northwestern coast of Egypt such as in Marabella, 6th of October resort, Edku Liquefied Natural Gas harbor (LNG), El-Arish power plant, El-Arish fishing harbor and along the Nile Delta, i.e. Rosetta Promontory **(Elsayed & Mahmoud, 2007)**. In addition to the afore- mentioned sites, Ras El Bar and Baltim are recognized **(Frihy & Lawrence, 2004)**. Moreover, it was noticed that groins are not effective in mitigating coastal erosion such as in the case of Burullus headland **(Elkafrawy *et al.*, 2020)**. Besides, they may create a weak circulation, causing water stagnation that adversely affect the water quality such as in El Asafra area in Alexandria **(Iskander *et al.*, 2007)**.

The hard structures are amongst the reasons for changing the shoreline behavior and disrupting the general alongshore erosion/accretion pattern **(Dewidar & Frihy, 2010)**. One of the disadvantages of groins is causing beach sediment starvation since they interrupt the longshore drift. On the other hand, soft coastal protection solutions, including sand nourishment and living coastal protection have been recently used in some Mediterranean coastal regions of Egypt.

Recently, remotely sensed (RS) data and geographical information system (GIS) have been providing valuable preliminary estimates of the shoreline change to understand the full processes related to the coastal erosion, deposition and response to protection means, and hence appropriate mitigation measures are recommended. Several studies have been carried out to assess the rates of the shoreline changes along the Nile Delta using (RS) and (GIS). Conversely, limited studies have focused on the Northwestern coast **(Iskander *et al.*, 2008; Iskander & Kut, 2014; Iskander, 2021; El-Masry *et al.*, 2022)**.

The goal of the present study was to assess the regressive and transgressive displacement of the shoreline along Agami−Sidi Kerair coastal" Pilot" area over 25 years to validate and compare the effectiveness and protection role of three different types of hard engineering structures applying (RS), (GIS) and (DSAS).

2. MATERIALS AND METHODS

2.1 Study area

The study area is located to the west of Alexandria city, extending for about 17.5 km from Agami Headland (E) to Sidi Kerair (W) (Fig. 1). This site was chosen as a pilot area for te current study due to the existence of three different types of hard structures

established to protect oil terminal harbor, urban and touristic areas. The main economic activities in the study area are manifested by the existence of ports, sea pipeline and cables, recreation, tourism, agriculture, wetlands and fisheries.

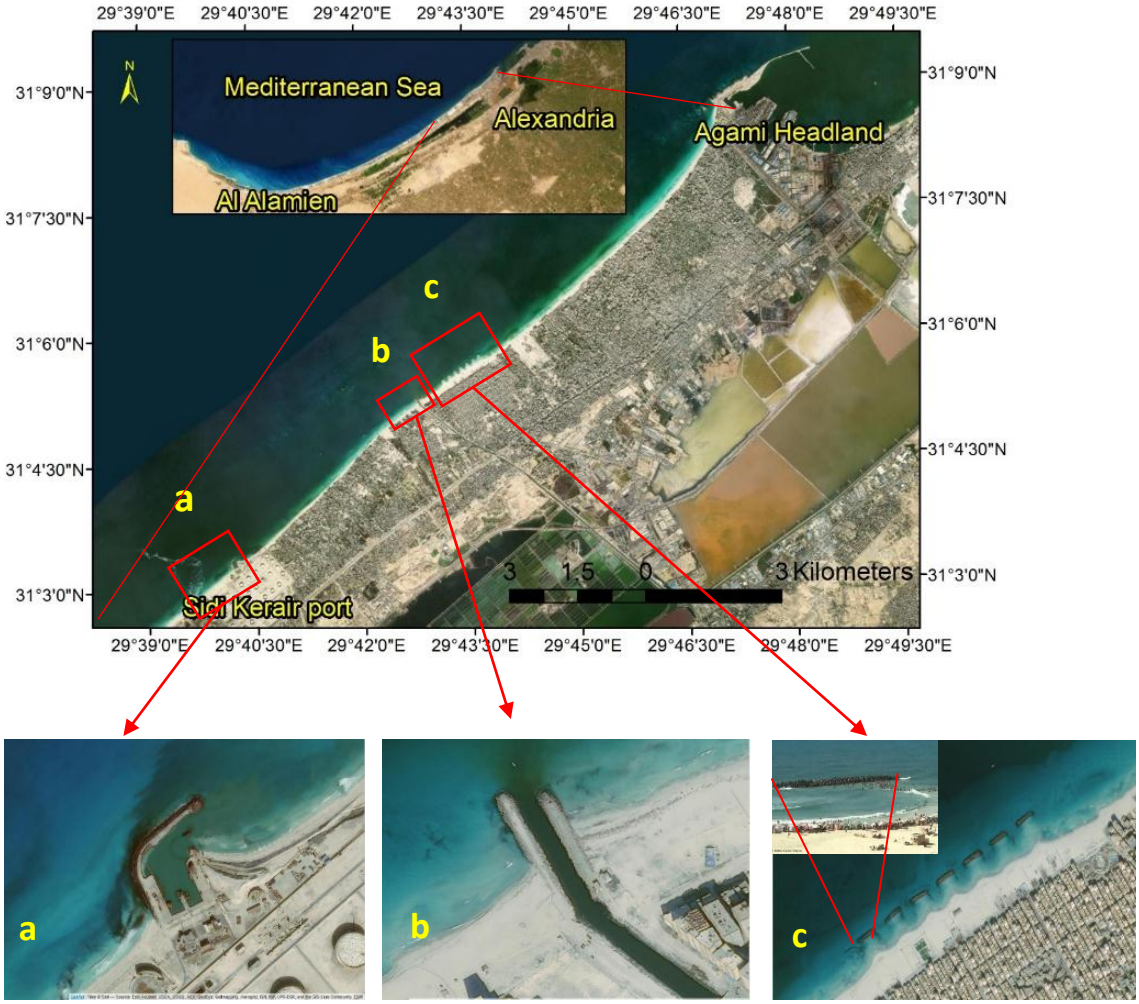

Fig. 1. Study area showing the location of three types of hard engineering structures **(a:** (SUMED) oil terminal harbor breakwaters connected to the shore; **(b**: Pairs of Nobaria Drain jetties, and **(c:** Seven emerged detached breakwaters at 6th of October beach

2.1.1 Dynamics

The nearshore bottom of the area has relatively gentle gradients, whereas the offshore is very steep (with a very narrow or missing continental shelf). The shore or coast, is mostly sandy, with a relatively wider beach **(Iskander *et al.*, 2007)**. Most of the sand is transported from eroded and disintegrating limestone ridges running parallel to the coastline in the backshore as well as of marine origin.

The average significant wave height and period are 1.04 m and 6.2 s, respectively, with a maximum wave height of 4.45m blown from NW in winter at the study site. During winter, the N, NNW, and NW waves cause morphological changes due to their long duration. In general, most of the predominant wave components propagating from NW, WNW, and W sectors are responsible of the generation of longshore currents towards the northeast (70% of wave distribution). Contrarily, the waves' approach from NNW, N, NNE, and NE generate a reverse long-shore current towards the southwest (19% of wave distribution). The remaining generally represents calm conditions with S and SE waves (11% of wave distribution) **(Iskandar *et al.*, 2007)**.

2.1.2 Protection structures

Three hard engineering protection structures were identified in the study area (Fig. 1) as follows:

a. Breakwaters: The Arab Petroleum Pipe Company (SUMED) has constructed two breakwaters connected to the shore at Sidi-Kerair oil terminal port (40 km west of Alexandria). These breakwaters extend seaward to a distance ranging between 150 and 250 m. The port is used to anchor small vessels serving the offshore loading of oil tankers by crude oil transferred to the Mediterranean Sea from the Gulf of Suez (via pipeline). These structures cause sedimentation and erosion problems in their updrift and downdrift zones **(Frihy, 2001)**.

b. Nobaria Drain jetties: The western Nobaria drain outlet is about 20 km to the west of Alexandria. Two jetties, each of which with length of 65 m, were constructed in 1986 to protect the drain exit from siltation **(Fanos *et al.*, 1995)**.

c. The 6thof October resort detached breakwaters: Seven dolos emerged detached breakwaters were built between 1998 and 2003 to provide a safe and secure area for swimming activities. Each breakwater is 100 m in length and 200 m away from the shoreline (at a depth between 4 and 5 m), leaving a 50 m gap between every two breakwaters. A crest level of +1.0 m referenced to MSL was adopted to force the wave energy of the storms **(Iskander *et al.*, 2007)**. Before their construction, the sea was not suitable for swimming due to hazardous rip currents, yet the problem still exists. The beach of this area was classified among the reflective and moderately dissipative beaches **(Nafaa & Frihy, 1993)**.

2.2 Data and Methodology

2.2.1 Methodology

The methodological approach to achieve the goal of the present study is shown in Fig. (2). This approach was adopted to assess the transgressive-regressive movements and detect the rates of shoreline change.

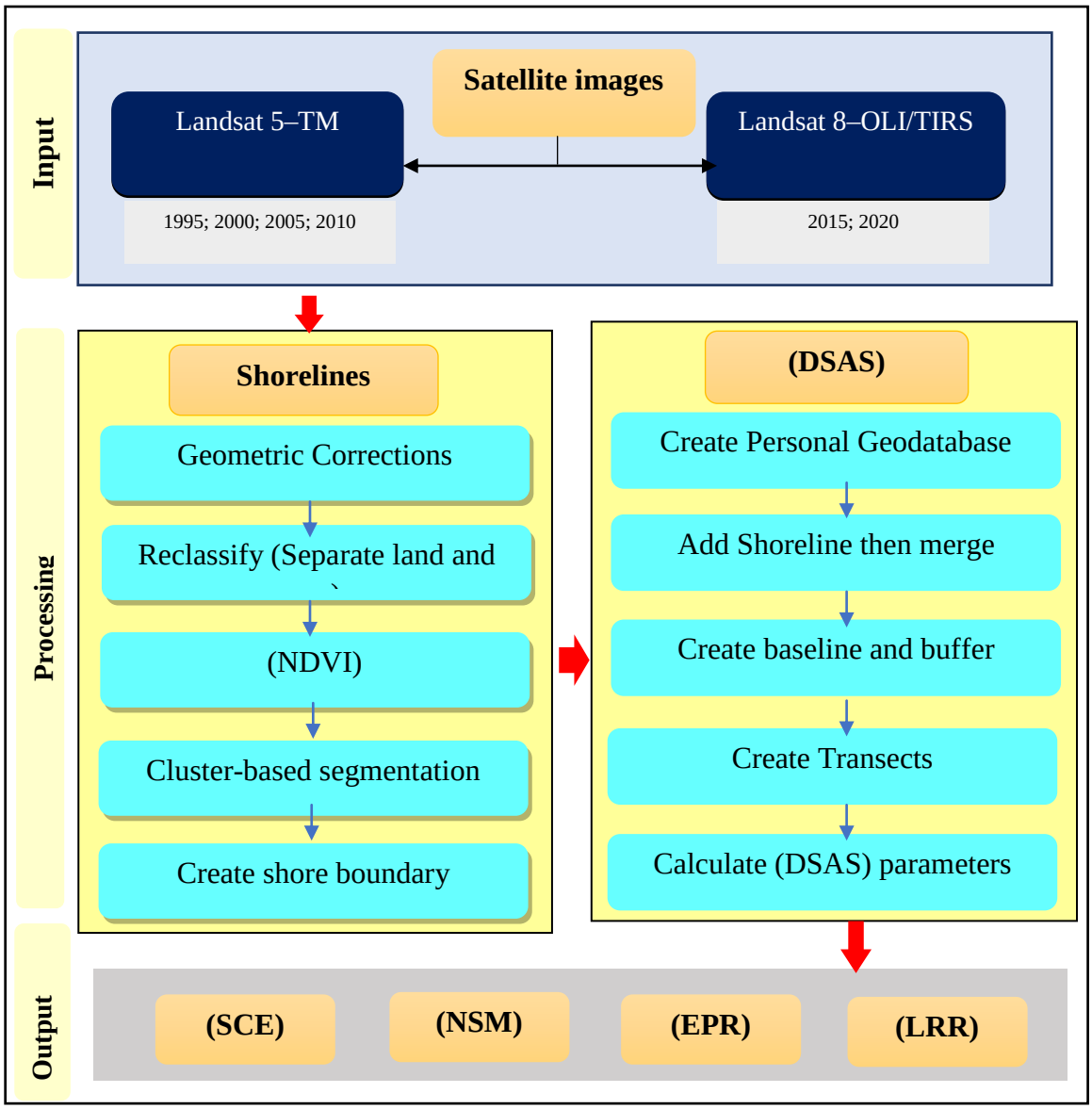

Fig. 2. Flowchart of the adopted methodological approach

2.2.2 Landsat images and extraction of the shoreline displacement

i) Landsat images

Four Landsat TM (1995, 2000, 2005, and 2010) and two Landsat OLI/TIRS (2015 and 2020) satellite images were used to study shoreline dynamics along Agami/Sidi–Kerair coast during 1995–2020, covering a period of 25 years. Images were downloaded from https://earthexplorer.usgs.gov/ (Table 1). All images were projected in WGS_84_UTM_zone_35N. Landsat 5 (TM) images consist of 7 spectral bands with a spatial resolution of 30 m for Bands (1–5, 7), while Landsat 8 images consist of 9 spectral bands with a spatial resolution of 30 m for Bands (1–7, 9).

ii) Image processing

All the scenes acquired in the spring season are of good quality and free of cloud (over the study area), addingly they are free of sensor defects such as striping and banding. Geometric correction interpretation depended basically on the digital Satellite map, forming a base map to Landsat image in 2020.

Table 1. Selected information of the acquired Landsat dataset

Year	Name of Satellite/Sensor	Path/Row	Date (dd/mm/yy)	Cloud cover	Spatial resolution (m)
1995	Landsat 5 (TM)	178/38	26/04/1995	0.00	30
2000	Landsat 5 (TM)	178/38	09/05/2000	0.00	30
2005	Landsat 5 (TM)	178/38	17/06/2005	0.00	30
2010	Landsat 5 (TM)	178/38	02/03/2010	0.00	30
2015	Landsat 8 (OLI/TIRS)	178/39	17/04/2015	0.00	15
2020	Landsat 8 (OLI/TIRS)	178/39	25/05/2020	0.00	15

Shoreline extraction

Although shoreline is simply defined as the physical interface of land and water, the shoreline delineation is one of the most critical, complex, and challenging processes due to the dynamic nature of factors determining its position **(Boak & Turner, 2005)**. The most common shoreline indicator is named by numerous authors as the High-Water Line (HWL) for it can be visible in the field and easily photo-interpreted **(Zhang *et al.*, 2002)**. In this context, the (HWL) was digitized in the current study using ArcGIS by manually tracing dry/wet line on the high-resolution satellite image of the study area extracted from Google Earth images for the year 2020 used for validating automatically extracted shorelines.

For the shoreline extraction, after the images processing, the boundaries of the study area were achieved by cropping the Landsat images. Determining the Normalized Difference Vegetation Index (NDVI) in this technique uses a composite red band and Near Infrared (NIR) to determine the level of greenness and classification of vegetation areas. The next step uses Tasseled Cap to convert the band channel into a new band set, for shoreline extraction. The Tasseled Cap was calculated according to the methods of **Crist (1985)** and **Chen *et al.* (2014)** for Landsat 5-TM and Landsat 8-OLI/TIRS images, respectively. The tasseled Cap process uses composite bands of red, green, blue, NIR, short wave infrared-1 (SWIR-1) and short-wave infrared-2 (SWIR-2) to find out the level

of brightness, greenness, and the wetness of an object. At the classification stage, to separate land from sea (NDVI) values, with respect to brightness, greenness, and wetness in this stage, pixel values were classified into two classes; namely, land class with value 0 and sea class with value 10 **(Natih *et al.*, 2020**). The next step is shore boundary, which is applied to make a shoreline from two classes of data using majority filtering, contours, and smooth line command **(Daniels, 2012)**. The last step is overlaying the shoreline extracted from the images to be furtherlt used for Digital Shoreline Analysis System (DSAS) to monitor the coastal processes and estimate the eroded/accreted zones.

Digital Shoreline Analysis System (DSAS)

Digital Shoreline Analysis System (DSAS) is a freely available toolbox extension to ESRI ArcGIS v.10 that calculates rate-of-change statistics from multiple historic shoreline positions through vector data **(Thieler *et al.*, 2009)**. The study created a hypothetical baseline buffered 150m from the shoreline position for the year 2020. This work carried out the shoreline analysis along 15.350 km through which (DSAS) cast 307 transects (T) orthogonal to the baseline at 50m intervals to intersect the 6 shoreline vector layers. The entire coastline was divided into 6 zones according to the characteristics of each zone and its response to the established hard protection structures as follows (Fig.3):

- Zone 1 extends for 0.5 km (from T#1 to T#10)
- Zone 2 extends for 5 km (from T#11 to T#110)
- Zone 3 extends for 2 km (from T#111 to T#150)
- Zone 4 extends for 4.9 km (from T#151 to T#248)
- Zone 5 extends for 1.7 km (from T#249 to T#282)
- Zone 6 extends for 1.3 km (from T#283 to T#307)

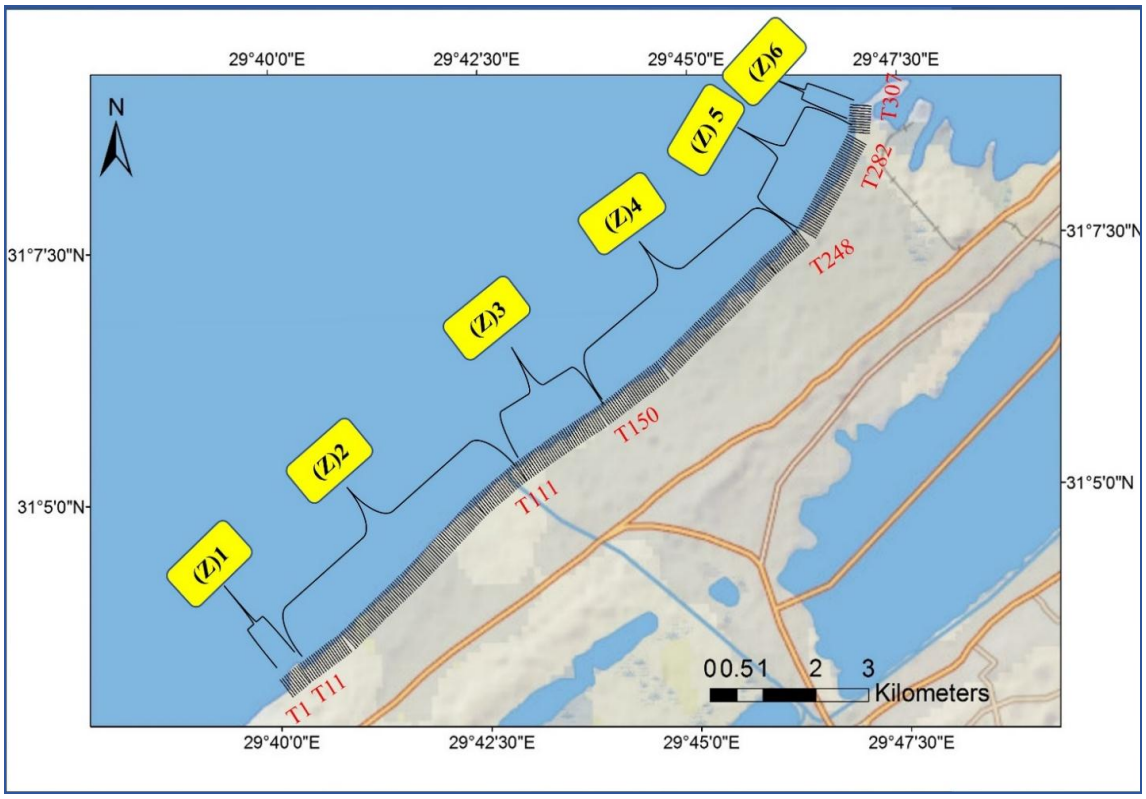

Fig. 3. Agami−Sidi Kerair coast layout (during 2020) showing transects (T) generated by the DSAS tool incorporated within ArcGIS software

Estimation of the shoreline changes along the coast of the study area was performed for a long-term period extending from 1995 to 2020. Furthermore, five short-term time intervals (1995–2000, 2000–2005, 2005–2010, 2010–2015, and 2015–2020) were considered to assess the impact of the coastal protection structures, which have significant effects (erosion/accretion) on shoreline dynamics.

The present study used two approaches in estimating the shoreline changes for both long-term and short-term changes; namely, the transect-based and the area-based approaches. The transect variation was assessed by computing the change in shoreline displacement and the rate of shoreline change, whereas the areal change was quantified by the variation in the beach area between these transects. For the landward recession (erosion), negative (−) symbols were assigned, whereas positive (+) symbols indicated seaward migration (accretion).

i. Transect-based approach

In this study, the following statistical methods were followed to calculate the shoreline displacement for each transect (Table 2) as follows:

a) The shoreline change envelope (SCE) is the distance between the shoreline farthest from and closest to the baseline at each transect. This represents a total change of shoreline displacement in terms of (erosion/accretion) distance without reference to their specific dates **(Oyedotun, 2014; Mullick *et al.*, 2020)**.

b) The net shoreline movement (NSM) estimates the distance between the oldest and the youngest shorelines in the meter unit **(Bheeroo *et al.*, 2016)**. In addition, it shows the direction of the displacement either towards the sea (accretion) or towards the land (erosion). When using two shoreline layers, the results of SCE resemble NSM **(Emam & Soliman, 2020)**.

c) The endpoint rate (EPR) is the rate that was calculated by dividing the net movement by the time elapsed in the oldest and the youngest shoreline in every transect in meter per year unit (**Ayadi *et al.*, 2016**). Besides, it converts the (NSM) into an annual rate of shoreline change.

d) The linear regression rate (LRR) represents the slope of a least-square straight-line, fitted through the shoreline positions at the various available times and it tends to underestimate/overestimate the rate of shoreline change relative to the (EPR) value **(Yasir *et al.*, 2020)**.

In the present study, long-term changes were presented by (SCE) and (NET) for the shoreline displacement, while the rate of shoreline change was displayed by (EPR) and (LRR). On the other hand, due to using merely two layers, the intermediate periods were presented by (NSM) for shoreline displacement and (EPR) for the shoreline displacement rate.

ii. Area-based approach

The study created six polygons for the whole study period (1995-2020); one for each zone, and then they were subtracted from each other to analyze the magnitude of short-term and long-term spatial changes (amounts of erosion and accretion) along the six studied zones.

Table 2. Definitions and/or methods of calculations of (DSAS) parameters employed in the present study

Parameter		Equation	Variables	Reference
The s shoreline Displacement (m)	(SCE)	Sd=df−dc	• S_d is a shoreline change distance (m). • df is the distance between baseline and farthest shoreline (m) at a particular transect (x_n). • dc is the distance between the baseline and closest shoreline (m) at the same above transect (x n).	**(Bheeroo *et al.*, 2016)**
	(NSM)	Snm=fo−fy	• *Snm* is the net movement of the shoreline (m). • f_o is the distance between baseline and shoreline (m) in	**(Bheeroo *et al.*, 2016)**

			the oldest date at a particular transect (x_n). • fy is the distance between baseline and shoreline (m) in youngest date at the same above transect (x_n).	
Rate of shoreline displacement (m/y)	(EPR)	EPR= (D1 – D2) / (t1 – t0)	• $D_1 - D_2$ is the distance (m) separating the latest and oldest shoreline. • $t_1 - t_0$ is the time interval (year) of the two shoreline positions.	**(Ayadi *et al.*, 2016)**
	(LRR)	Y= a + bx	• *y* is the distance (m) from the baseline. • *a* is the cutoff of *y*. • *b* indicates the slope of the linear regression line that represents the shoreline change rate. • *x* indicates shoreline position in different years.	**(Ayadi *et al.*, 2016)**

3. RESULTS AND DISCUSSION

3.1 Analysis of shoreline changes

A total of 307 transects covering a shoreline length of about 15.350 km were obtained to measure shoreline changes in the study area for the long-term period (25 years, 1995−2020), applying (SCE), (NSM), (EPR), and (LRR) to estimate change/change rate statistics (Figs.4-10). Fig. (4) shows the (SCE) results during the study period (1995−2020), changing from 2.5 m at zone 3 (T#307) to 151 m at zone 5 (T#249) with an average value of 45.6 m.

The (NSM) results for the period (1995−2020) are represented in Fig. (5), and the overall shoreline change (Fig. 6) indicates that the different segments of the shoreline in the study area showed different variability during the last three decades. Beach accretion and sediment deposition were high at the landward direction of the coastal constructions. The shoreline of zones 1, 3, and 5 showed gradual accretion, while zones 2, 4, and 6 experienced erosions for the period (1995−2020). The total number of transects that shows accretion is 232, representing approximately 75.57% of the shoreline of the study area, which covers a total length of 11.6 km. The length of the shoreline experiencing erosion is 3.75 km, which is much lower than the accreted parts, comprising about 24.43% of the study area measured along 75 transects. The (NSM) values for the study period (1995–2020) reached a maximum value of 80 m at zone 3 (T#139) and a minimum value of -68.34 at zone 6 (T#303). Results of (NSM) for the intermediate periods are

(1995–2000 (Fig. 7a), 2000–2005 (Fig. 7b), 2005–2010 (Fig. 7c), 2010–2015 (Fig. 7d) and 2015–2020 (Fig. 7e)). These results show a predominant accretion at all zones for the last two intermediate periods of (2010−2015) and (2015−2020), reaching a maximum value of 69.97 m at zone 6 (T# 239). For the intermediate periods lying between 1995 and 2000 (before construction of the 6th of October resort detached breakwaters), the shoreline showed great stability along 172 transects, which extended about 8.6 km (56 % of the total shoreline length). About 287 transects that extended for 14.35 km along the study area experienced erosion in the intermediate period (2000−2005), which would be attributed to the disturbance in sediment transport that occurred due to the construction of the 6th of October resort detached breakwaters. Generally, the results indicate that the shoreline of the study area has a dynamic sediment transport with marked alternation between erosion and accretion, which is in accordance with results obtained from other studies **(Iskander *et al.*, 2007*;* Iskander & Kut, 2014)**.

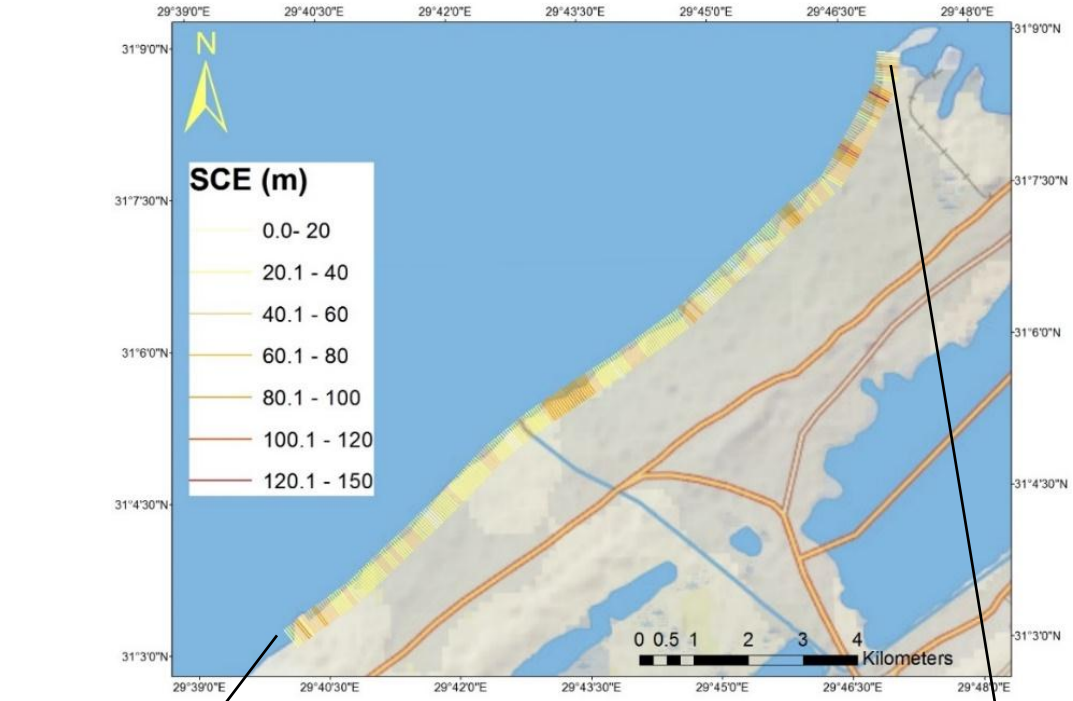

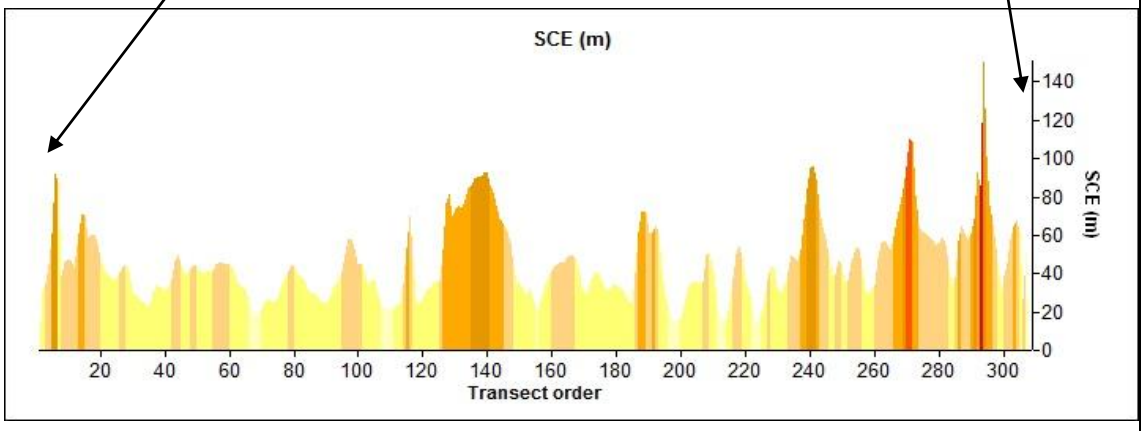

Zone No.		**Z1**	**Z2**	**Z3**	**Z4**	**Z5**	**Z6**
(**ESC**) (m)	Min.	30.68	18.44	23.29	14.02	33.69	2.50
	Max.	92.66	71.63	93.42	96.35	150.99	68.34
	Average	53.08	37.49	58.87	40.68	69.27	46.67
No. of Transects		10	100	40	98	34	26

Fig. 4. Shoreline change envelope (SCE) of the study area

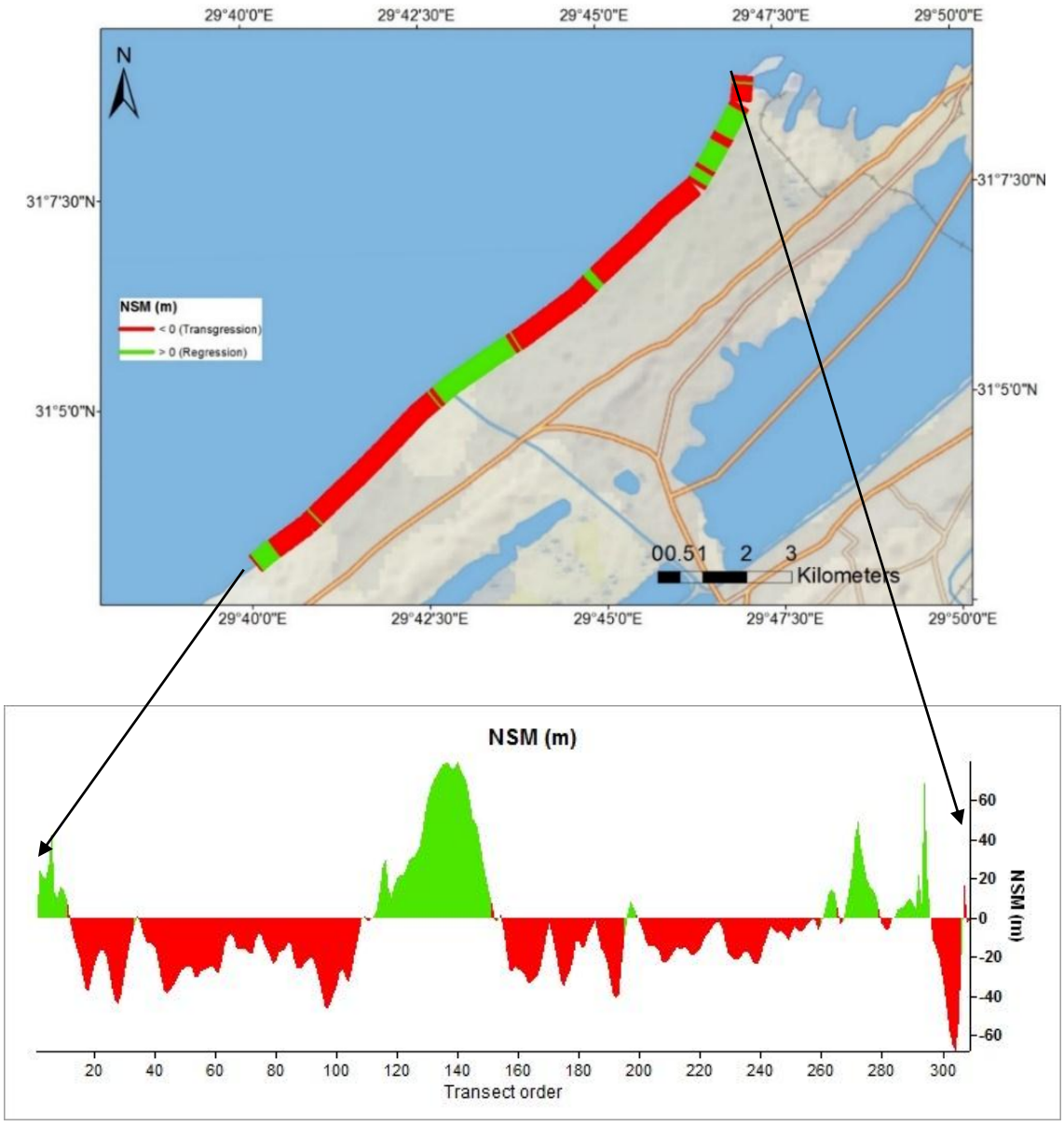

Zone No.		Z1	Z2	Z3	Z4	Z5	Z6
(**NSM**) (m)	Min.	7.44	-46.32	0.59	-40.76	-6.49	-68.34
	Max.	42.95	1.57	79.99	8.74	69.26	0.00
	Average	19.98	-21.93	43.51	-15.05	14.00	-32.67
No. of Transects		10	100	40	98	34	26

Fig. 5. Net shoreline movement (NSM) of the study area

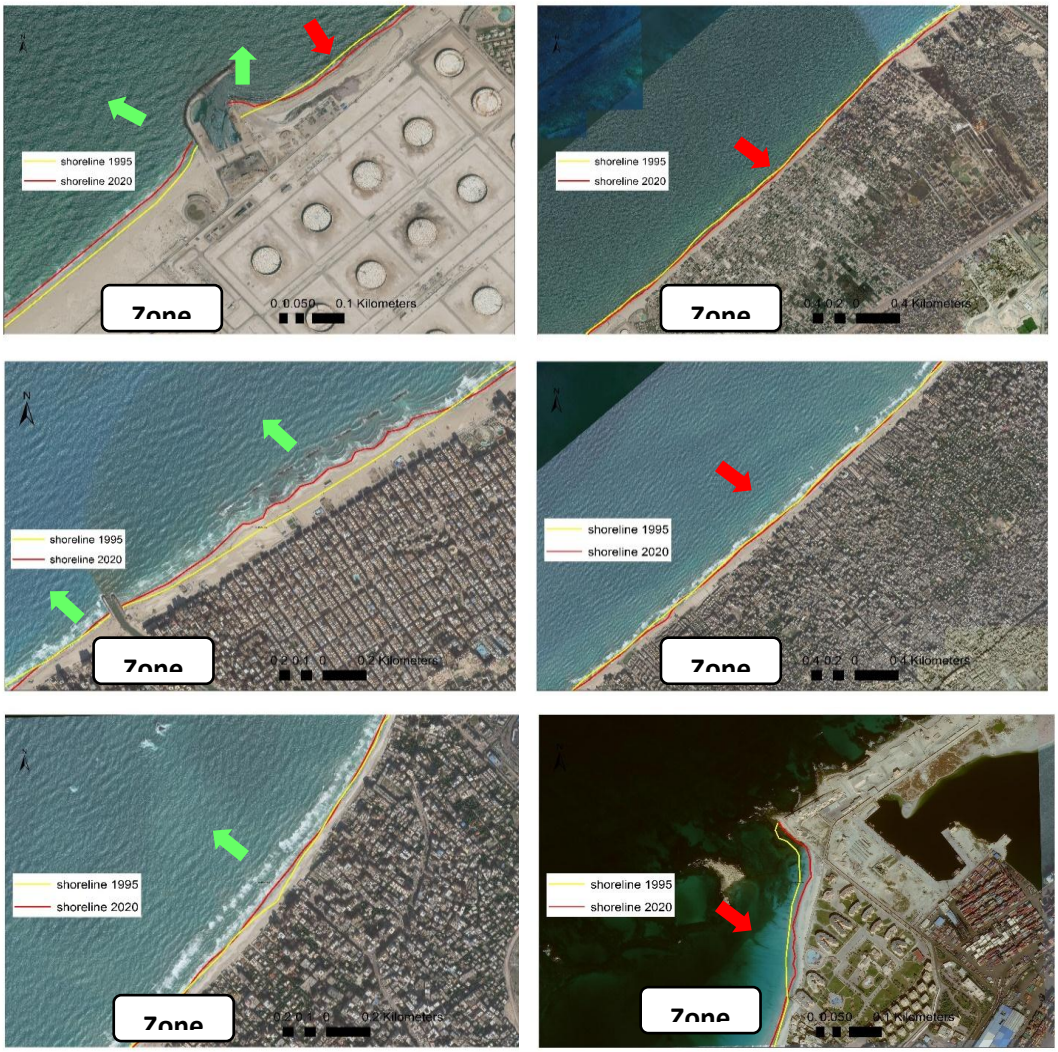

(-ve value: erosion; +ve value: accretion)

Fig. 6. Overall shoreline displacement from 1995 to 2020
(Red arrow: Erosion and Green arrow: Accretion)

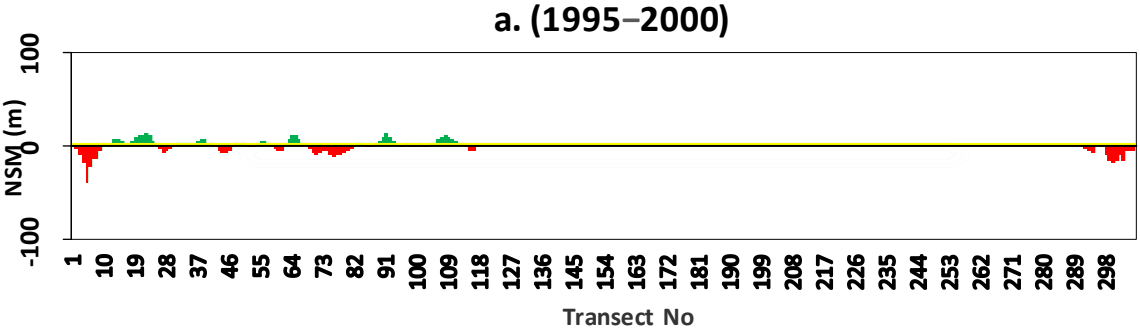

Zone No.	Z1	Z2	Z3	Z4	Z5	Z6

(**NSM**) (m)	Min.	-21.72	-11.48	-6.62	0.00	0.00	-17.84
	Max.	0.86	13.46	5.80	0.00	0.00	0.00
	Average	-11.05	-0.05	-0.11	0.00	0.00	-5.17

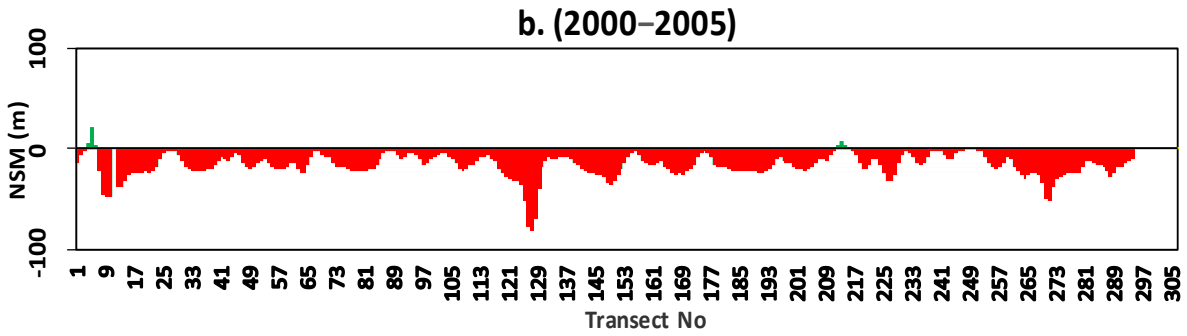

Zone No.		**Z1**	**Z2**	**Z3**	**Z4**	**Z5**	**Z6**
(**NSM**) (m)	Min.	-47.45	-37.11	-81.63	-80.35	-52.38	-26.90
	Max.	22.12	-0.39	-6.76	31.17	0.42	0.00
	Average	-14.99	-14.51	-24.80	-0.43	-20.66	-8.20

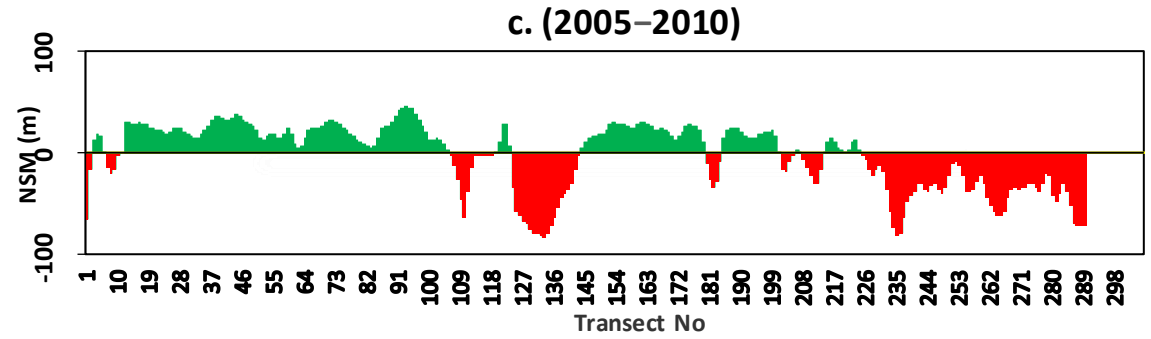

Zone No.		**Z1**	**Z2**	**Z3**	**Z4**	**Z5**	**Z6**
(**NSM**) (m)	Min.	-65.37	-64.18	-82.25	-80.35	-62.14	-82.24
	Max.	19.77	45.69	28.61	15.28	-8.50	0.00
	Average	-8.48	21.22	-25.12	-23.49	-34.97	-16.13

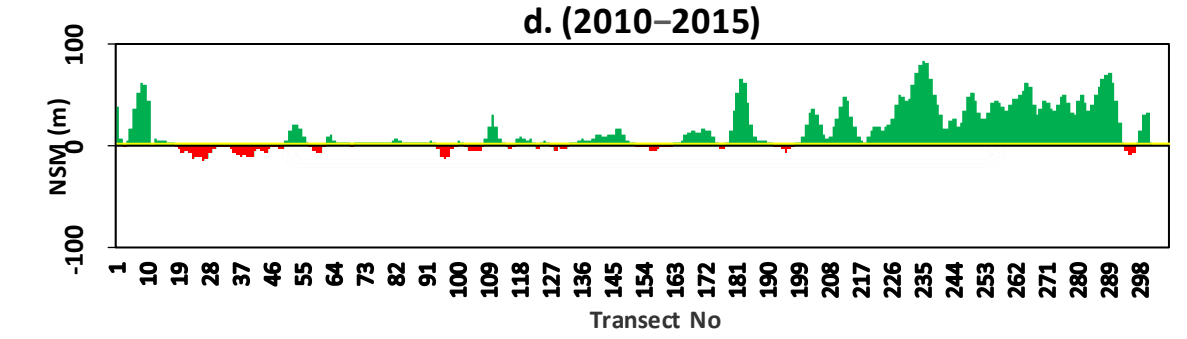

Zone No.		**Z1**	**Z2**	**Z3**	**Z4**	**Z5**	**Z6**
(**NSM**) (m)	Min.	-1.31	-15.32	-4.78	-7.27	25.10	-9.19

	Max.	60.74	30.01	17.36	83.17	61.09	69.97
	Average	31.17	-0.80	4.16	19.44	40.89	22.80

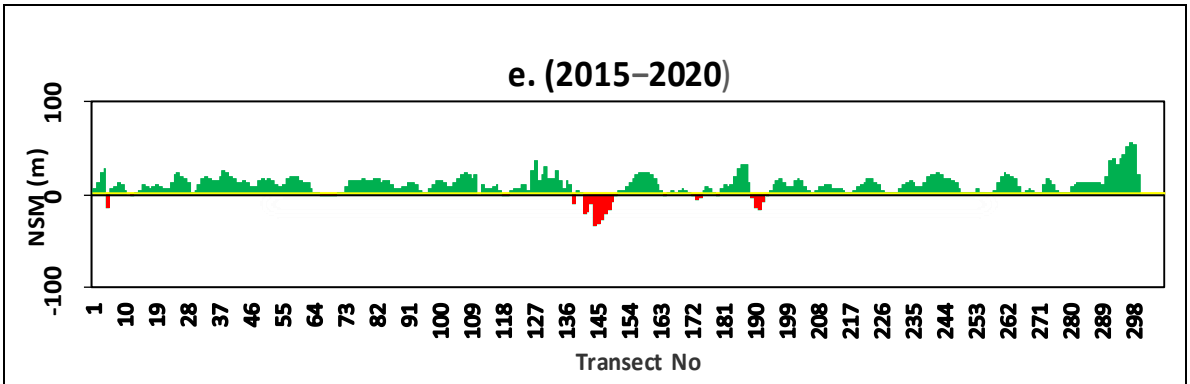

Zone No.		Z1	Z2	Z3	Z4	Z5	Z6
(**NSM**) (m)	Min.	-14.13	-0.97	-34.03	-17.28	0.79	0.00
	Max.	28.65	25.02	36.12	32.93	23.46	55.07
	Average	9.95	12.13	3.32	9.62	7.93	19.25

Fig.7. Descriptive statistics of the (NSM) for the four intermediate periods **(a)** 1995–2000; **(b)** 2000–2005; **(c)** 2005–2010; **(d)** 2010–2015, and **(e)** 2015–2020

The results of the graphical and the statistical evaluation of (LRR) and (ERR) showed that they provide practically the same rates (Figs. 8, 9). The (LRR) values are presented in Fig. (8). It was noted that the minor variation in this parameter was observed throughout the study area during the study period. The maximum (LRR) value is 4.30 m/year, while the minimum value is -2.57 m/year at zones 3 and 6, respectively. As shown in Figs. (8, 9), the results of (EPR) and (LRR) for the period from 1995–2020 introduced a close similarity, which coincides with the findings of **Nassar *et al.* (2019)** and **Awad and El-Sayed (2021)**. Therefore, there was no need to use the two methods Simultaneously. In the present study, (EPR) was selected for evaluating the rate of shoreline changes of the study area. The spatial changes in the shoreline of the study area were determined using the rates calculated by (EPR) for the four intermediate periods (1995–2000 (Fig. 10a), 2000–2005 (Fig. 10b), 2005–2010 (Fig. 10c), 2010–2015 (Fig. 10d) and 2015–2020 (Fig. 10e)).

The change rates of the same zone of the shoreline were generally comparable for the whole study period between 1995 and 2020. The change rates of the same zone differed with a change 4 m/year for the four periods of this study. They were slightly higher than those obtained in the study period between 1995 and 2020.

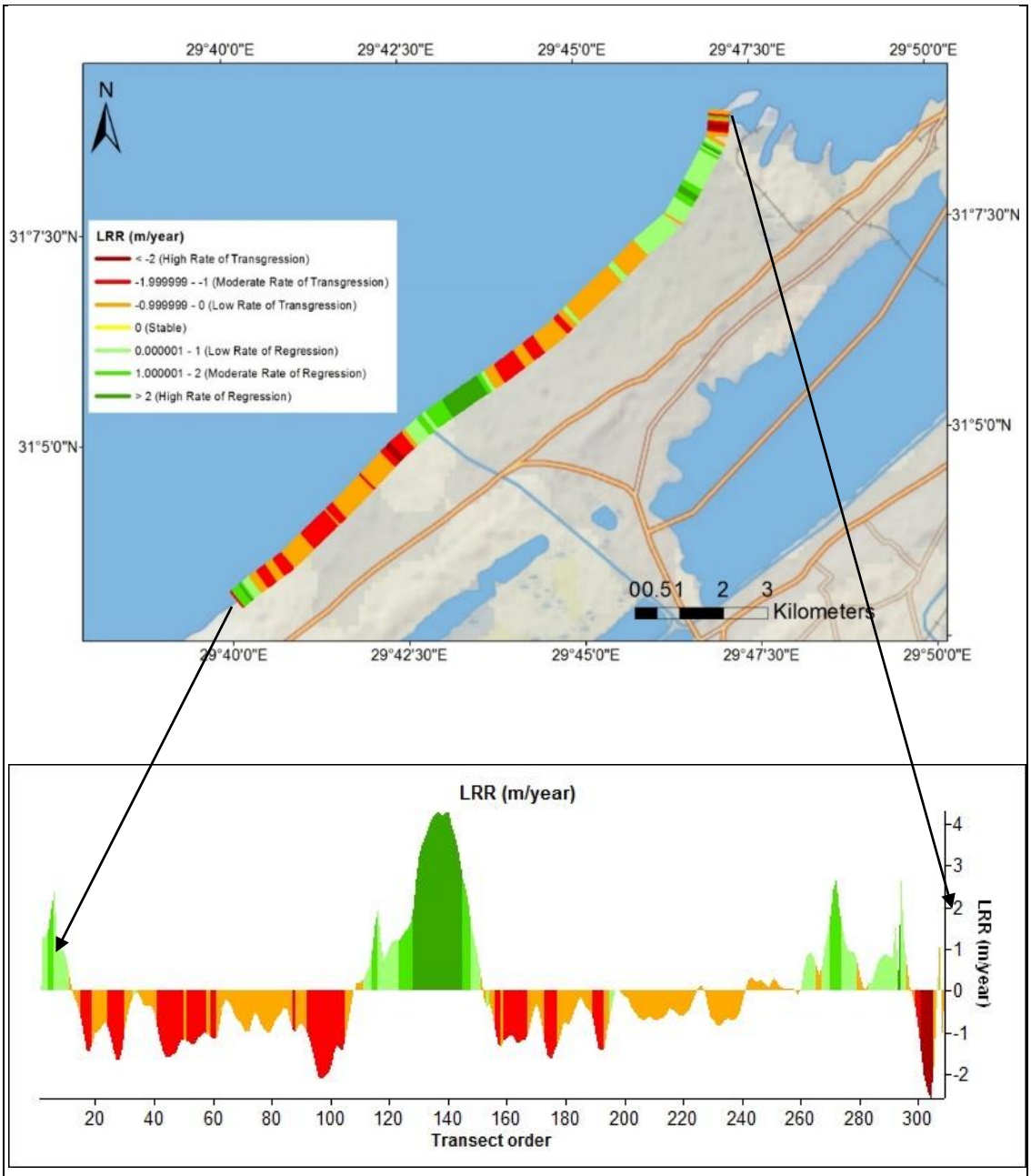

Zone No.		Z1	Z2	Z3	Z4	Z5	Z6
(**LRR**) (m/year)	Min.	0.36	-2.11	0.35	-2.57	0.06	-2.57
	Max.	2.40	0.30	4.30	0.37	2.66	0.12
	Average	1.28	-0.90	2.31	-0.51	1.00	-1.07
No. of Transects		10	100	40	98	34	26

Fig. 8. Linear Regression Rate (LRR) (1995 and 2020)
(-ve value: erosionand; +ve value: accretion)

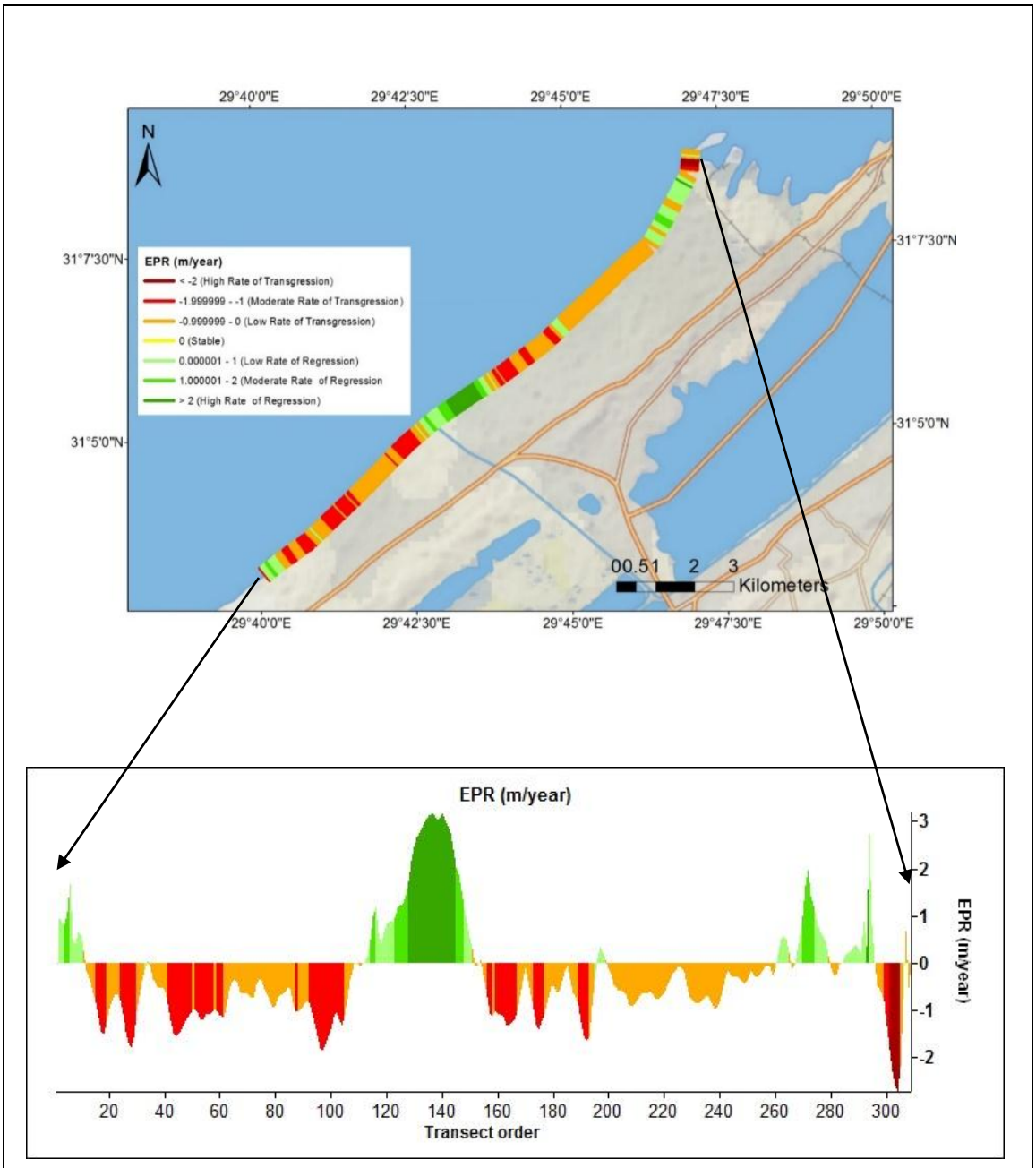

Zone No.		Z1	Z2	Z3	Z4	Z5	Z6
(**EPR**) (m/year)	Min	0.30	0.00	0.02	-1.63	-0.26	-2.72
	Max	1.71	-0.03	3.19	0.35	2.76	0.00
	Average	0.80	-0.88	1.74	-0.59	0.56	-1.34
No. of Transects		10	100	40	98	34	26

Fig. 9. End Point Rate (EPR) of the study area between 1995 and 2020
(-ve value: erosion; +ve value: accretion)

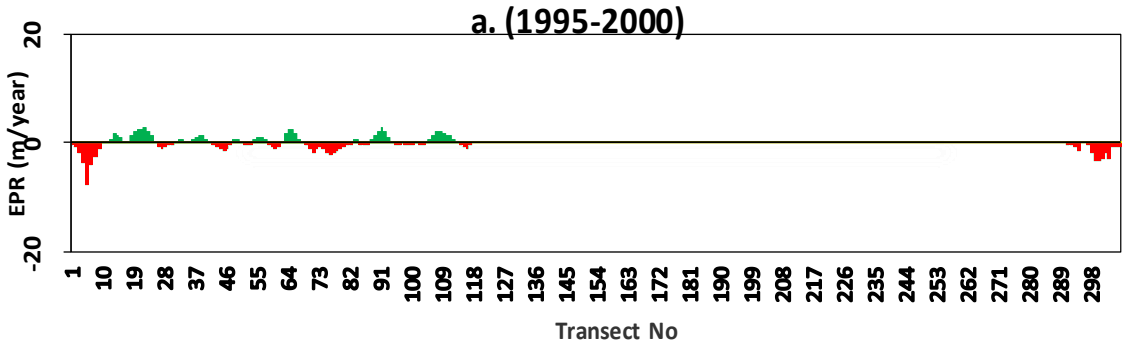

Zone No.		Z1	Z2	Z3	Z4	Z5	Z6
(**EPR**) (m/year)	Min.	-4.34	-2.30	-1.25	0.00	0.00	-3.57
	Max.	0.17	2.69	1.16	0.00	0.00	0.00
	Average	-2.21	0.24	-0.02	0.00	0.00	-1.03

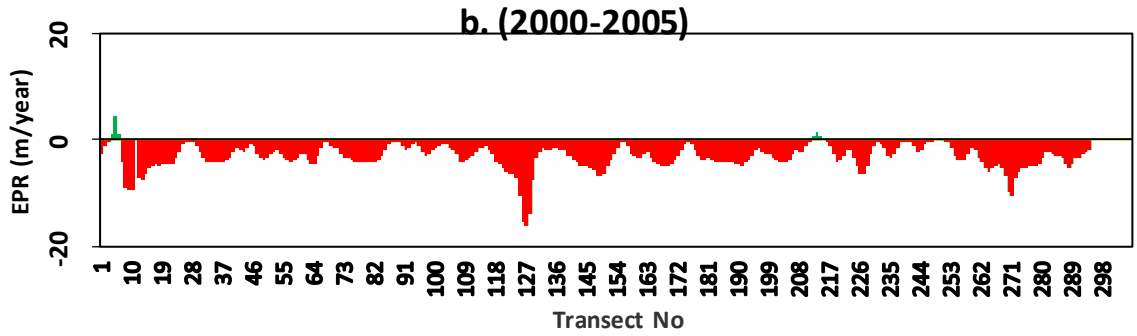

Zone No.		Z1	Z2	Z3	Z4	Z5	Z6
(**EPR**) (m/year)	Min.	-9.49	-7.42	-16.33	-6.54	-10.48	-5.38
	Max.	4.42	-0.08	-1.35	1.40	0.08	0.00
	Average	-3.00	-2.90	-4.96	-2.70	-4.13	-1.64

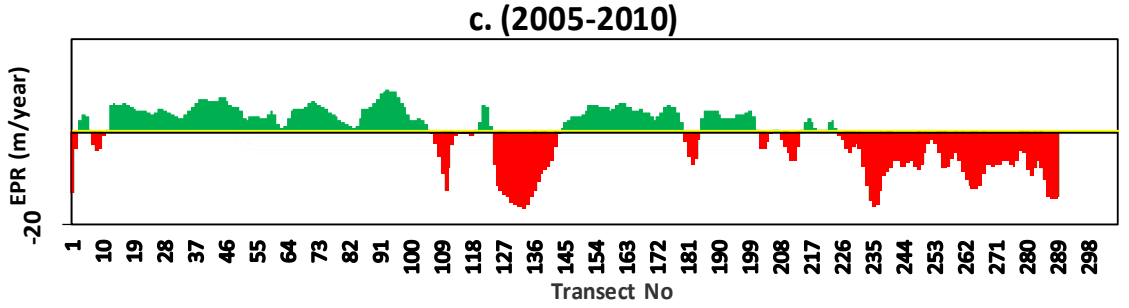

Zone No.		Z1	Z2	Z3	Z4	Z5	Z6
(**EPR**) (m/year)	Min.	-13.07	-12.84	-16.45	-16.07	-12.43	-14.45
	Max.	3.95	9.14	5.72	6.23	-1.70	0.00
	Average	-1.70	4.24	-5.02	-0.09	-6.99	-3.23

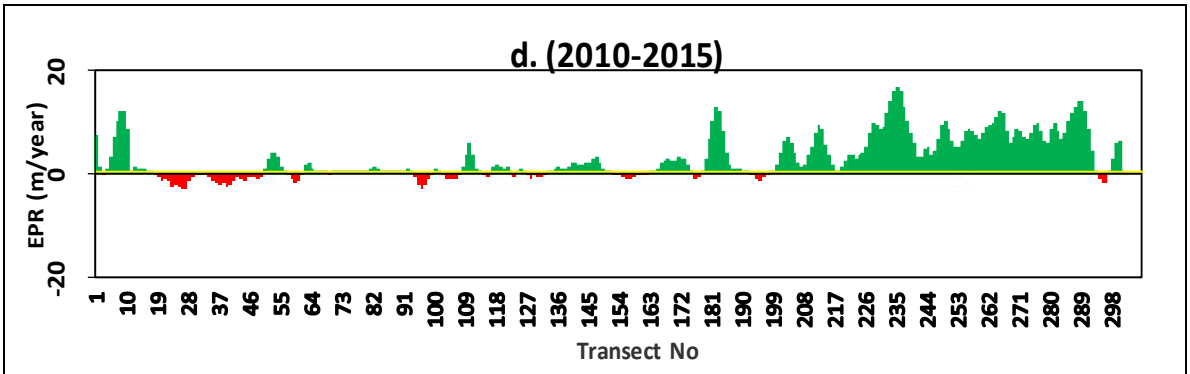

Zone No.		Z1	Z2	Z3	Z4	Z5	Z6
(**EPR**) (m/year)	Min.	-0.26255	-3.06	-0.96	-1.45	5.02	-1.84
	Max.	12.14743	6.00	3.47	16.63	12.22	13.99
	Average	6.23323	-0.16	0.83	3.85	8.18	4.56

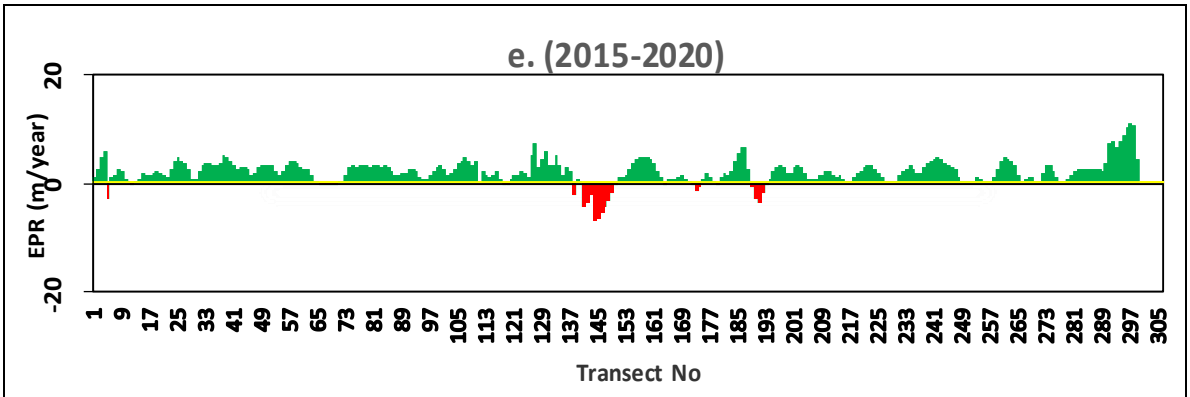

Zone No.		Z1	Z2	Z3	Z4	Z5	Z6
(**EPR**) (m/year)	Min.	-2.83	-0.19	-6.81	-3.46	0.16	0.00
	Max.	5.73	5.00	7.22	6.59	4.69	11.01
	Average	1.99	2.43	0.66	1.90	1.59	3.85

Fig.10 Descriptive statistics of the (EPR) for the four intermediate periods **(a)** 1995–2000; **(b)** 2000–2005; **(c)** 2005–2010; **(d)** 2010–2015 and **(e)** 2015–2020

The detailed results of the shoreline analysis for each zone were as follows:

Zone 1 is the shortest section in this study, covering only a shoreline length of 500 m along the coast of Sidi Kirair port. As presented in Fig. (7), average (NSM) results showed an erosion process that occurred during the first three intermediate periods (1995-2000, 2000-2005 and 2005-2010). It reached a maximum value of -65.36 m during (2010-2015). On the other hand, (NSM) results showed the last two intermediate periods (2010−2015 and 2015−2020); this zone underwent an accretion process and the (NSM) reached 60.74 m during (2010 −2015). During the study period (1995-2020), the shoreline experienced a maximum (SCE) and (NSM) values at (T#5), which were 92.66 m and 42.95m, respectively. The high accretion rate is related to the presence of (SUMED) western breakwater, which trapped sand on the western sides (Fig. 6). A moderate deposition took place on the eastern side of the eastern breakwater at (T#9),

with (SCE) value of 47.2 m and (NSM) value of 15.2 m. Minor accretion was observed at (T#8) in the center of the entrance of the port, with (NSM) value of 10.45m. This phenomenon may be due to the repeated dredging of the sediment from the jetty entrance failing to remedy the problem. The shoreline displacement rate represented by (EPR) recorded negative average values in the intermediate periods before 2010, which had dominant erosion reaching a maximum value of -13.07 m/year in the period from 2005–2010. Accretion occured along zone 1 in the other two periods in 90% of the transects, reaching a maximum value of 12.15 m/year in the period from 2010–2015. The accretion rates of two periods (2010–2015, 2015–2020) vary between 5.73 m/year which occurred in the 2015–2020 period, and 12.17 m/year which happened in 2010–2020 period. The maximum accretion rate for the long-term period (1995–2020) of this zone was 1.71 m/year. This zone is also classified as a moderate erosion zone for the total period of the study, recording an average (EPR) value of 0.80 m/year (Fig.9).

Generally, this zone was in an accretion state during the study period at all transects. These observations are agreeable with those of **Frihy (2001)** who stated that, the relatively high rate of accretion in harbors may be attributed to the deposition of sediments that cause undesirable shoaling in the entrance of the port.

Zone 2 is the longest zone in the study area, comprising about 32.5 % of its shoreline. It stretches about 5 km from Sidi Kirair for (E) to "Nobaria drain outlet" (W), including "Abu Talat" beach. This zone showed varied changes in its shoreline movement between the different intermediate periods, including erosion and accretion. However, erosion occured along this zone for the intermediate period (1995−2000) on a very limited number of transects and at a very low value without exceeding - 0.05 m, which is virtually negligible. The erosion increased in the following intermediate period of 2000−2005 and recorded an average (NSM) value of -14.51m. In the 2005−2010 period, this zone was under the influence of the accretion process, and the (NSM) reached a maximum value of 45.69 m, with few numbers of transects (5%) undergoing erosion at the eastern side (T#105−T#110), reaching -64.18 m with an average value of 21.22 m. In the intermediate period (2010−2015), a very limited erosion was observed reaching an average (NSM) value of 0.08m. The accretion increased to reach a maximum (NSM) value of 25.2 m and an average value of 12.13 m. This is less than the accretion of the intermediate period of (2005−2010).

For the long-term period (1995−2020), as shown in Fig. (4), (SCE) values ranged from 18.44m at (T#68) and 71.63m at (T#13), with an average of 37.49m. A gradual decrease was detected in (SCE) values eastward. The (NSM) had negative values at all transects (erosion), with an average value of -21.93m, a maximum value of -46.32m at (T#96) and a minimum value of -1.57 at (T#34). This high erosion process would be attributed to the disturbance of the hydrodynamic system due to the presence of (SUMED) breakwaters that disrupt the eastward littoral sediment transport.

Zone 3 stretches for about 2 km and covering about 13.02 % of the study area shoreline. It starts from the western "Nobaria drain outlet" to the eastern side of the 6th of October resort. This zone has two kinds of protection structures; jetties and emerged detached breakwaters. The shoreline displacement change of this zone switched from general erosion during the intermediate periods (1995−2000, 2000−2005, and 2005−2010) to accretion in the successive periods of this study (2010−2015 and 2015−2020). The average erosion in the first three intermediate periods reached -25.12 m in the period (2005−2010). This accretion started to increase on most of the transects of this zone that started during the intermediate period (2010−2015) for about 75%, and receded in the next intermediate period (2015−2020) to record a percentage of 67.5 of all transects. Accordingly, average (NSM) values decreased from 4.16 m to 3.32 m for the intermediate periods (2010−2015) and (2015−2020), respectively.

The overall results of the study time (1995−2020) indicate that the shoreline of this zone records the highest accretion process among the six studied zones. The maximum value of (NSM) was 79.99 m at (T#139) between the third and fourth emerged breakwaters, and the average (NSM) value was 43.51 m. A minimum accretion was recorded in the west side of the western jetty of "Nobaria Drain" at (T# 111), with (NSM) value of 0.59m. Moderate accretion value was spotted in the east part of the eastern jetty (T#120), recording a value of 22.12 m. Since the western jetty interrupts the eastern sediment transport, sedimentation was observed. The recorded accretion is high behind detached breakwaters. Presently, these detached breakwaters were effective in mitigating the erosion and creating a narrow swash-aligned coastline with a typical "zig-zag" shoreline Fig. (6). Nevertheless, the beaches are not suitable for swimming due to the steep slope of their surf zone and the generation of rip currents that cause several troubles and serious hazards for the swimmers.

Zone 4 covers a shoreline length of 4.9 km and comprises about 31.9% of the shoreline of the study area, including "Abo-Youssif ", "Hannovil" and "Bitash" areas. This zone is exposed to the sea without protection means. In the intermediate period (1995−2000), the shoreline of this zone was in a stable state with no shoreline displacement. The temporal changes started in the 2000–2005 period, with an average (NSM) value reaching -0.43 m and increased to -23.49 m during the intermediate period (2005−2010). The shoreline movement of this zone was abruptly reversed to complete accretion in the (2010−2015) period with an average (NSM) value of 19.44 m, and it decreased to 9.62 m in the next period (2015−202).

For the whole study period (1995−2020), this area recorded a maximum (NSM) value of 8.74 m (EPR: 0.35 m/yr.). This zone eroded with an average (NSM) value of -15.05 m (EPR-0.59 m/yr.) and a maximum erosion at the western side of this zone, with a maximum (NSM) value of -40.76 m (EPR: -1.63 m/yr.). This has occurred due to the negative impact of the 6thof October detached breakwaters; the rapidly formed tombolos

in the shadow zone of those breakwaters that have blocked the sediment flow to the east, and thus contributed to beach erosion at the downdrift side of these structures **(Frihy, 2001)**.

Zone 5 shoreline is about 1.7 km, representing 31.8% of the shoreline of the study area. It has the same displacement pattern (stable, erosion, and accretion) of the previous zone for the intermediate periods though over shorter shoreline lengths. It started by having a stable shoreline for all transects as indicated by its displacement change for the 1995–2000 period (Fig. 7-a,). Erosion started in most of the transects (94%) of this zone, with an average (NSM) value of -20.66 m in the 2000–2005 period. This erosion increased in the next period (2005−2010) to attain an average (NSM) value of -34.97 m. The shoreline displacement change switched back in the intermediate periods (2010–2015) and (2015−2020) to include dominant accretion and few or negligible erosion transects.

Zone 6 is the last section in the study area, which is located on its eastern end of the shoreline of the study area. It is the second shortest zone which represents "Agami Headland", with a 1.3 km shoreline covering 8.4 % of the shoreline of the study area. It has the same pattern displacement pattern of zone 1 and 3, which was dominated by erosion in the first three periods and witnessed a widespread accretion in the last two periods. Erosion gradually increased during the first three intermediate periods; hence, average recorded (NSM) values were -5.17 m, -8.20 m, and -16.13 m in the intermediate periods (1995−2000), (2000−2005) and (2005−2010), respectively. Accretion started in the period (2010−2015), and the shoreline displacement reached 22.80 m. The accretion continued in the last intermediate period (2015−2020) but with a slight decrease in the average (NSM) value recording 19.25 m.

For the long-term period (1995−2020), this zone showed the highest erosion rates compared to the others. It suffers from erosion with an average (NSM) value of -32.67 m (EPR: -1.34 m/yr.) and the maximum erosion reaches 68.34 m (NSM) (EPR: -2.72 m/yr.).

3.2 Evaluation of beach area (erosion/accretion) and proposed protection means

The gains or losses of the beach sediments (accretion and erosion) relative to the shoreline change were expressed in terms of surface area for the whole study period (1995-2020). About 211.275 m2 of beach area showed a remarkable loss, while about 119.985 m2 of the beach area was expanded. The maximum area of beach loss of about -103.462 m2 was noticeable in Zone 2 (Fig. 11). The most significant accretion was recorded at zone 3 as the beach gained 89.354m2. When the spatial shoreline changes, the sand loss or gain shows a successive accretion (beach gain) and erosion (beach loss) trend along the study area with an overall erosion trend. Therefore, the effect of the existing hard structures is detrimental in the study area. Despite their detrimental consequence as they transfer the erosion problem to the adjacent areas, disturb sediments supply, and accelerate the confined bottom erosion causing downdrift scouring. This is attributed to their effect as a barrier to the longshore sediments transport. In addition to the afore-

mentioned negative consequences, the generation of the hazardous rip current and the increasing risk on swimmers are considered.

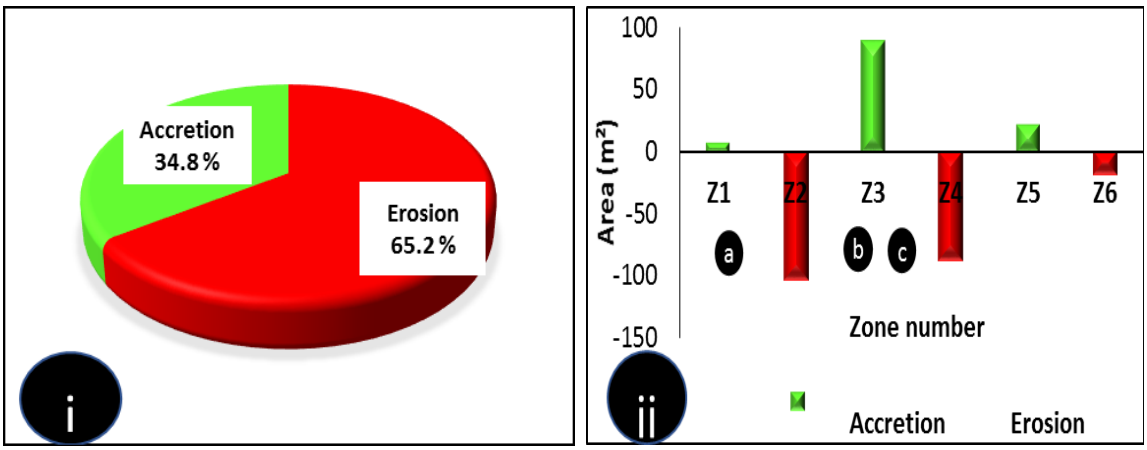

Fig. 11. i) The percentage of total erosion/accretion of the study area over 25 years. **ii)** The beach area per zone erosion /accretion (25 years) showing **a**: Location of Sidi-Kerair port breakwaters; **b**: location of Nobaria pair of jetties and **c**: Location of 6thof October detached breakwaters

4. CONCLUSION

During the study period, the beach has experienced erosion with different beach segments despite the hard engineering structures. Thus, the maximum recorded coastal erosion/accretion kinematics are -2.72/+3.19 m/year for zones 3 and zone 6, respectively. Regardless of the consequences on beach amenity and aesthetics, the emerged detached breakwaters proved their effectiveness in protecting the shoreline from erosion and building up the beach area. However, jetties and breakwaters failed in solving other problems related to the recreational purpose of the beach rather than erosion. Consequently, the existing hard structures in the study area failed to solve the problem completely or even mitigate the erosion in the entire area. Conversely, they conveyed the problem from one place to another. Furthermore, adverse impacts can thus arise from both the protection structures themselves, as well as human responses to the impacts. Conclusively, this study, therefore, draws the attention of all stakeholders to develop and adopt an immediate shoreline management plan for the area between Agami headland and Sidi-Kerair considering the response of the shoreline. In addition, "soft" protection methods which are becoming more prevalent in coastal areas need to be incorporated in conjunction with traditional "hard" coastal structures or newly developed techniques to attain the target.

Recommendations: Based on the afore-mentioned results, the present study recommends:

1- Installation of submerged breakwaters at both sides efficiently blocks longshore currents reducing the chance of rip currents occurrence instead of the detached emerged breakwaters at zone 3.

2- Applying innovative hybrid techniques such as beach nourishment alongside hard structures as means of reducing the erosion at zones 4 and 6.

REFERENCES

Awad, M. and El-Sayed, H.M. (2021). The analysis of shoreline change dynamics and future predictions using automated spatial techniques: Case of El-Omayed on the Mediterranean coast of Egypt. Ocean Coast. Manag., 205(1): Article 105568. https://doi.org/10.1016/j.ocecoaman.2021.105568.

Ayadi, K.; Boutiba, M.; Sabatier, F. and Guettouche, M.S. (2016). Detection and analysis of historical variations in the shoreline, using digital aerial photos, satellite images, and topographic surveys DGPS: case of the Bejaia bay (East Algeria). Arab. J. Geosci., 9: 1–12.

Bheeroo, R.A.; Chandrasekar, N.; Kaliraj, S. and Magesh, N.S. (2016). Shoreline change rate and erosion risk assessment along the Trou Aux Biches–Mont Choisy beach on the northwest coast of Mauritius using GIS-DSAS technique. Environ. Earth Sci., 75: 1–12.

Boak, E.H. and Turner, I.L. (2005). Shoreline definition and detection: A review. J. Coast. Res., 21: 688–703.

Crist, E.P. (1985). A TM Tasseled Cap equivalent transformation for reflectance factor data. Remote Sens. Environ., 17: 301–306.

Daniels, R.C. (2012) Using Arcmap to Extract Shoreline from Landsat TM and ETM+. In Proceedings of the Thirty-Second ESRI International Users Conference, San Diego, CA, USA, 12–16 July, 2012, 23pp.

Dewidar, K.M. and Frihy, O.E. (2010). Automated techniques for quantification of beach change rates using Landsat series along the North-eastern Nile Delta, Egypt. J. Oceanogr. Mar. Sci., 1: 28–39.

El-Masry, E.A.; El-Sayed, M.K.; Awad, M.A.; El-Sammak, A.A. and El Sabarouti, M.A. (2022). Vulnerability of tourism to climate change on the Mediterranean coastal area of El Hammam–EL Alamein, Egypt. Environ. Dev. Sustain., 24(1): 1145–1165. https://doi.org/10.1007/s10668-021-01488-9.

El Sayed, W. R. and Khalifa, A.M. (2017). NILE Delta shoreline protection between past and future. Twentieth International Water Technology Conference, IWTC20, Hurgada, Egypt, 18-20 May, 2017, pp.18–20.

Elkafrawy, S.B.; Basheer, M.A.; Mohamed, H.M. and Naguib, D.M. (2020). Applications of remote sensing and GIS techniques to evaluate the effectiveness of coastal structures along Burullus headland-Eastern Nile Delta, Egypt. Egypt. J. Remote Sens. Sp. Sci., 1–8.

Elsayed, M.A.K. and Mahmoud, S.M. (2007). Groins system for shoreline stabilization on the east side of the Rosetta promontory, Nile Delta coast. J. Coast. Res., 23: 380–387.

Emam, W.W.M. and Soliman, K.M. (2020). Applying geospatial technology in quantifying spatiotemporal shoreline dynamics along Marina El-Alamein Resort, Egypt. Environ. Monit. Assess., 192(7): 459–473. https://doi.org/10.1007/s10661-020-08432-w.

Fanos, A.M.; Khafagy, A.A. and Dean, R.G. (1995). Protective works on the Nile Delta coast. J. Coast. Res., 11: 516–528.

Frihy, O.E. (2001). The necessity of environmental impact assessment (EIA) in implementing coastal projects: Lessons learned from the Egyptian Mediterranean coast. Ocean Coast. Manag., 44: 489–516.

Frihy, O.E. and Lawrence, D. (2004). Evolution of the modern Nile delta promontories: Development of accretional features during shoreline retreat. Environ. Geol., 46: 914–931.

Iskander, M.M. (2021). Stability of the Northern coast of Egypt under the effect of urbanization and climate change. Water Sci., 35: 1–10.

Iskander, M.M. and El Kut, A.E.S. (2014). Beach Behavior and Impact of Coastal Structures on the Sustainable Development, Cases from the Northwestern Coast of Egypt. Open j. ocean coast. sci., 1(1): 12–24.

Iskander, M.M.; Abo Zed, A.I.; El Sayed, W.R. and Fanos, A.M. (2008). Existing marine coastal problems, western Mediterranean coast, Egypt. Emir. J. Eng. Res., 13 (3): 27–35.

Iskander, M.M.; Frihy, O.E.; El Ansary, A.E.; Abd El Mooty, M.M. and Nagy, H.M. (2007). Beach impacts of shore-parallel breakwaters backing offshore submerged ridges, Western Mediterranean Coast of Egypt. J. Environ. Manage., 85: 1109–1119.

Mullick, M.R.A.; Islam, K.M.A. and Tanim, A.H. (2020). Shoreline change assessment using geospatial tools: a study on the Ganges deltaic coast of Bangladesh. Earth Sci. Inform., 13: 299–316.

Nafaa, M.G. and Frihy, O.E. (1993). Beach and nearshore features along the dissipative coastline of the Nile Delta, Egypt. J. Coast. Res. 9(2): 423–433. https://www.jstor.org/stable/4298100?seq=1.

Nassar, K.; Mahmod, W.E.; Fath, H.; Masria, A.; Nadaoka, K. and Negm, A. (2019). Shoreline change detection using DSAS technique: Case of North Sinai coast, Egypt. Mar. Georesources Geotechnol. 37: 81–95.

Natih, N.M.N.; Pasaribu, R.A.; Sangadji, M.S. and Kusumaningrum, E.E. (2020). Study on shoreline changes using Landsat imagery in Sangsit Region, Bali Province. IOP Conf. Ser. Earth Environ. Sci. 429(1): Article 012059. https://doi.org/10.1088/1755-1315/429/1/012059

Oyedotun, T.D.T. (2014). Shoreline Geometry : DSAS as a Tool for Historical Trend Analysis. Geomorphol. Tech., 2: 1–12.

Thieler, E.R.; Himmelstoss, E.A.; Zichichi, J.L. and Ergul, A. (2009). Digital Shoreline Analysis System (DSAS) version 4.0 – An ArcGIS extension for calculating shoreline change. U.S. Geol. Surv. Open-File Rep. 2008-1278. https://doi.org/10.3133/ofr20081278

Yasir, M.; Sheng, H.; Fan, H.; Nazir, S.; Niang, A.J.; Salauddin, M. and Khan, S. (2020). Automatic Coastline Extraction and Changes Analysis Using Remote Sensing and GIS Technology. IEEE Access., 8: 180156–180170.

Zhang, K.; Huanj, W.; Douglas, B.C. and Leatherman, S.P. (2002) Shoreline position variability and long-term trend analysis. Shore Beach., 70 (2): 31.